SACLANTCEN MEMORANDUM
serial no.: SM-297

SACLANT UNDERSEA RESEARCH CENTRE MEMORANDUM

COMPARISON OF SATELLITE-RETRIEVED SEA-SURFACE TEMPERATURES WITH DRIFTER-AND SHIP-BORNE MEASUREMENTS

H.H. Essen, E. Nacini,
P. M. Poulain

January 1996

The SACLANT Undersea Research Centre provides the Supreme Allied Commander Atlantic (SACLANT) with scientific and technical assistance under the terms of its NATO charter, which entered into force on 1 February 1963. Without prejudice to this main task – and under the policy direction of SACLANT – the Centre also renders scientific and technical assistance to the individual NATO nations.

SACLANT Undersea Research Centre
Viale San Bartolomeo 400
19138 San Bartolomeo (SP), Italy

tel: +39-187-540.111
fax: +39-187-524.600

e-mail: library@saclantc.nato.int

NORTH ATLANTIC TREATY ORGANIZATION

Comparison of satellite-retrieved sea-surface temperatures with drifter- and ship-borne measurements

H.-H. Essen, E. Nacini, P.-M. Poulain

The content of this document pertains to work performed under Project 23 of the SACLANTCEN Programme of Work. The document has been approved for release by The Director, SACLANTCEN.

David L. Bradley
Director

intentionally blank page

Comparison of satellite-retrieved sea-surface temperatures with drifter- and ship-borne measurements

H.-H. Essen, E. Nacini, P.-M. Poulain

Executive Summary: In the context of rapid assessment of environmental parameters, satellite-measured sea-surface temperatures (SST) are of great value. SST is highly correlated with sound speed, knowledge of which can contribute to sonar performance prediction. The Advanced Very High Resolution Radiometers (AVHRR), which have been flying in the NOAA series of polar-orbiting weather satellites have provided such data since 1978. With two satellites in orbit, the swath of about 3000 km yields global coverage four times a day, even of regions which are inaccessible. The AVHRR maps large areas quasi synoptically with high resolution (up to 1 km), and the data are available nearly in real-time, e.g. onboard ship.

SACLANTCEN has been working with AVHRR data since 1980. Hard- and software have been developed for receiving Automatic Picture Transmission (APT) data onboard NRV *Alliance*. This transmission consists of two of the five AVHRR channels at a reduced resolution of about 4 km. In addition, High Resolution Picture Transmission (HRPT) data have been purchased for off-line analysis. With the recent interest in rapid assessment of coastal areas it became desirable to have an HRPT receiver onboard NRV *Alliance*. Commercial systems are now available, and SACLANTCEN has purchased a *TeraScan* system from SeaSpace Corp. (USA).

This memorandum investigates the accuracy with which SST can be retrieved from the satellite AVHRR measurements by means of the Centre's new *Tera-Scan* system. Ground-truth data from measurements onboard NRV *Alliance* and from satellite-tracked drifters are used. Most of the data are from the Mediterranean and some from the North Atlantic. It has been found that the accuracy of the global NOAA algorithm is better than 0.7°. In principle, higher accuracy may be obtained with regional algorithms

intentionally blank page

Comparison of satellite-retrieved sea-surface temperatures with drifter- and ship-borne measurements

H.-H. Essen, E. Nacini, P.-M. Poulain

Abstract: Sea-surface temperatures (SST) retrieved from satellite imagery are compared with *in-situ* measured data. The satellite data are from the Advanced Very High Resolution Radiometer (AVHRR) of the series of NOAA satellites, partly purchased from the University of Dundee (UK) or recorded by the new high-resolution receiver of SACLANTCEN, a *TeraScan* system (SeaSpace Corp., USA). Both data sets have been processed by the *TeraScan* software. The ground-truth data are from satellite-tracked drifters and from measurements onboard NRV *Alliance*. The aim of this memorandum is to determine the performance of the *TeraScan* system with respect to the accuracy of retrieved SST.

For reliably determining SST from the AVHRR, two steps have to be performed. First, cloud-contaminated data have to be removed and second, the measured brightness temperatures have to be corrected for atmospheric effects. The impact of these procedures on the accuracy of satellite-measured SST is investigated.

Keywords: Mediterranean – Nordic Seas – satellite imagery – sea-surface temperature – *TeraScan* system

Contents

1
Introduction

Sound-speed in the ocean is highly correlated with temperature. For this reason, activities in satellite remote sensing at SACLANTCEN have been concentrated on the infrared channels of the Advanced Very High Resolution Radiometer (AVHRR), from which sea-surface temperature (SST) can be determined. The AVHRR has been operated from the series of NOAA satellites since 1978. Hard- and software have been developed at SACLANTCEN for receiving Automatic Picture Transmission (APT) data on *NRV Alliance.* This transmission consists of two of the five AVHRR channels at a reduced resolution of about 4 km. With the recent interest in rapid assessment of coastal areas it became desirable to have a High Resolution Picture Transmission (HRPT) receiver on *NRV Alliance.*

Systems that allow the acquisition and processing of HRPT data in near real-time are now available. SACLANTCEN recently purchased the *TeraScan* system from SeaSpace Corp. (USA) for operation at the Centre and aboard *NRV Alliance.* This system has been installed at a number of fixed land sites or on research vessels. For example, Siegel *et al.* [1] analyse surface patterns in the Baltic Sea by means of AVHRR images acquired and processed with a *TeraScan* system.

The purpose of this memorandum is to investigate the performance of the *TeraScan* system with respect to the determination of SST. The largest limitation to the application of infrared satellite measurements to the measurement of SST is the presence of clouds. Areas, contaminated by clouds have to be identified and discarded for the SST-retrieval. In this memorandum we shortly describe the methods used by the *TeraScan* software.

Because of atmospheric effects brightness temperatures measured by the infrared channels do not correspond to temperatures at the sea surface. The largest error source in the computation of SST from infrared satellite imagery is the correction for signal attenuation by atmospheric water vapour. The standard multichannel algorithm (MCSST) uses the difference between two thermal infrared channels to correct for the thermal moisture effect. Channels 4 and 5, which share the atmospheric window at $10 - 13\mu m$, are the channels which are mainly considered. The retrieval methods are split-window algorithms, the coefficients of which are assumed to vary from satellite to satellite, and are different for day- and night-time imagery. Dependencies on viewing angle of the radiometer, mean water-vapour content of the atmosphere, region or season have been considered with some success.

Algorithms may be tuned in two different ways. The empirical approach is based on the collection of coincident *in-situ* measurements. The alternative approach simulates the satellite measurements for a large set of atmospheric profiles. The main disadvantage of the empirical method is that it compares different quantities, the so-called 'skin-temperature' of the uppermost 1 mm of the sea-surface, measured by the satellite, and the bulk-temperature of the ground-truth measurement at greater depths. The simulation model determines the skin temperature but is limited by insufficient knowledge of the atmosphere.

Extensive literature exists on the measurement of SST by means of space-borne radiometers, especially the AVHRR. We refer only to a very limited selection. The history of SST measurements with spaceborne radiometers from 1970 to 1985, the conceptual basis for cloud filtering and atmospheric attenuation correction, and MCSST procedures are given in [2]. Recently, Barton reviewed the historical development and the current status of techniques for deriving SST from satellite sensors, with emphasis on AVHRR [3]. A comparison of algorithms for deriving SST from the AVHRR shows that there has been little improvement in accuracy over the past decade. Using data for typical subtropical, midlatitude summer and winter conditions, Barton [3] compared the retrieved SSTs (at the nadir) from some 30 algorithms and found a standard deviation of the order of 0.4°C.

The application of different retrieval algorithms to the same satellite measurements may lead to results differing by up to 2°C [4]. The referenced paper compares both bulk- and skin-temperatures from the eastern Mediterranean (off Crete) with SSTs retrieved from the AVHRR of NOAA-11. The bulk temperatures were measured by thermistors from *NRV Alliance* at 0.1 m and 2 m depth, the skin temperatures by two airborne radiometers. The authors claim that at present there exists no algorithm that is universally accepted.

The present investigations are based on the split-window algorithm used by NOAA for the operational generation of SST maps [5]. The algorithm contains linear expressions of channel-4 and channel-5 brightness temperatures and a dependence on the radiometer look angle. The coefficients were determined by regressing satellite data with *in-situ* measurements from drifting buoys. Applying this algorithm, we determine the accuracy of SST retrieval with different sets of ground-truth data (bulk temperatures) measured from *NRV Alliance* in the Mediterranean (Tyrrhenian and south Adriatic Sea), and satellite-tracked buoys in the Mediterranean (Adriatic and Ionian Sea) and in the Nordic (Greenland-Iceland-Norwegian) Seas. In order to investigate the performance of the algorithms, slightly modified versions are considered with the coefficients determined from the data available.

2
Satellite data

The satellite data used are from the Advanced Very High Resolution Radiometer (AVHRR), carried on the NOAA series of satellites. These satellites operate in a near-polar, sun-synchronous orbit of about 102 min duration, which corresponds to 14.1 orbits per day. With two satellites in orbit, the swath of about 3000 km yields global coverage four times a day. The pixel size of the AVHRR is 1.1×1.1 km^2 at the surface point degrading to 1.5×4.0 km^2 at the swath edges.

2.1 *Advanced Very High Resolution Radiometer*

The AVHRR is a five-channel device, operating in the visible, 0.62 μm (channel-1), 0.91 μm (channel-2), and infrared, 3.7 μm (channel-3), 10.8 μm (channel-4), 12.0 μm (channel-5). Visible data values may be converted to albedos (ratio of reflected to incident solar radiation). The percent albedo is computed as a linear function of the input data. In the context of our investigations this value is of interest for detecting clouds.

The infrared channels are in the so-called atmospheric window where the atmosphere is relatively transparent. Channel-4 and channel-5 share the same window with wavelengths close to the peak of the Planck function for terrestrial temperatures. The thermal data values may be converted to temperatures. The radiance measured by the sensor is computed as a linear function of the input data values [5],

$$E_i = S_i C_i + I_i, \tag{1}$$

where E_i is the radiance and C_i the input data value (0 - 1023 counts) of channel $i = 3, 4, 5$. The calibration coefficients S_i (slope) and I_i (intercept) can be determined from measurements of an onboard black body calibration target and the space radiation from the direction away of the sun. These values are provided for each scan of the AVHRR, and vary slightly during a satellite overpass. The conversion to brightness temperature $T_i[^\circ K]$ from radiance E_i is performed by using the inverse of Planck's radiation equation,

$$T_i = \frac{C_2 \nu_i}{ln(1 + C_1 \nu_i^3 / E_i)}, \tag{2}$$

where C_1 and C_2 are constants, and ν_i are the central wave numbers of the channel response function. The spectral response functions differ slightly from satellite to satellite and are provided by NOAA.

2.2 TeraScan system

The *TeraScan* system at SACLANTCEN uses a 0.46 m HRPT flat-plate tracking antenna. The antenna is specifically designed to operate aboard ship, automatically compensating for roll and pitch. Gyro compass input is needed to correct for the ship's course. A GPS antenna is part of the system, providing accurate time and location. The configuration consists of two antennas, one mounted on *NRV Alliance*, the other installed on the roof of the institute. For most of the time, the receiver and the processing computer are attached to the antenna at the Centre, and only occasionally taken to the ship.

The *TeraScan* system includes a software package for the acquisition, calibration, display, and manipulation of images from spaceborne instruments. The HRPT-images are received in real-time from the satellite. The positioning of the antenna is based on an orbital prediction model. To ensure that the antenna accurately tracks the satellite and for accurate pass processing, it is necessary to regularly update a set of orbital parameters for each satellite. With these data, a table of satellite predictions may be generated, which is based on the position of the receiving station. The AVHRR raw data are converted into albedo or brightness temperature. The calibration coefficients in equation (1) are provided by the *TeraScan* software for each 100 input lines during a satellite overpass.

2.3 Cloud masking

Reliable values of SST can only be obtained from areas that are sufficiently cloud-free. Based on the work of McClain et al. [2], the *TeraScan* software package offers a variety of tests to identify and eliminate cloudy or unreliable data. Thresholds for different parameters can be chosen. Only pixels that pass all tests are considered for the determination of SST. The tests make use of channel-4 and channel-5 and also of the visible channel-2, which is available only during daytime, and of the infrared channel-3 for night-time data. For some of the tests, the pixel under consideration is embedded at the center of a box of 3×3 pixels. These boxes are used for two purposes, to suppress noise by averaging over the pixels in the box, and to detect small-scale cloud contamination by comparing adjacent pixels. The tests and reasonable thresholds are:

Tests applicable to both day- and night-time data:

1) Pixels are removed if the channel-4 brightness temperature T_4 is below a certain threshold, determined by the climatology of the area under consideration.

2) Because of the increasing path length, data from the edges of the swath are of low quality. Usually, pixels viewed under zenith angles greater than 60^o are discarded.

3) A pixel, considerably cooler than the adjacent ones, may be contaminated by small clouds. If, within the box, the absolute difference of T_4 at any pixel and the center pixel exceeds a certain value, e.g. 0.3^oC, the pixels are eliminated.

Test applicable to daytime data only:

4) If the channel-2 albedo exceeds a given value, e.g. 5%, the pixel is discarded. This test eliminates areas contaminated by sunglint or clouds.

5) Small clouds may also affect the albedo. If, within the box, the absolute difference of the channel-2 albedo at any pixel and the center pixel exceeds a given value, e.g. 0.3%, the pixels are eliminated.

Test for night-time data only:

6) The pixel is discarded if the difference between the brightness temperatures of channel-3 and channel-4 is less than a threshold of e.g. -1.5^oC. Because of the noisiness of the channel-3 data this test is applied to the means over the pixels in the box.

2.4 SST retrieval

Brightness temperatures retrieved from the infrared channels do not correspond to the water temperatures at the sea surface, because of atmospheric effects. The most important atmospheric constituent for reducing the radiation temperature for channel-4 and channel-5 is water vapour. The atmospheric transmission spectra have various dependencies at different wavebands, even within quite narrow spectral intervals. This spectral dependence implies that coincident measurements at different channels can be used to correct for the atmosphere.

In general, the brightness temperature measured by the satellite underestimates the SST. The deficit depends primarily on the air-sea temperature difference. Statistics of this value may show seasonal variability [6]. Since the atmosphere is less transparent for channel-5 than channel-4 , T_5 is generally cooler than T_4.

The most frequently used method to retrieve the real sea-surface temperature T_S from the AVHRR data is by means of a split window algorithm, which uses the difference between the brightness temperatures of channel-4 and channel-5 to correct for the atmospheric effects. These algorithms provide the greatest accuracy, as they do not use channel-3 data, which can have random noise of up to 1.5^oC. The simplest split window algorithm is,

$$T_S = a_o + a_1 T_4 + a_2(T_4 - T_5). \tag{3}$$

Due to different spectral response curves the coefficients (a_o, a_1, a_2) vary from satellite to satellite. In general, different values are also used for day- and night-time. For physical reasons it can be expected that the coefficients are not constant, as assumed by (3), but depend on the atmospheric water vapour content and on the look angle of the radiometer, which determines the path length through the atmosphere.

Emery *et al.* [7] discuss the influence of the water vapour and suggest the retrieval algorithm,

$$T_S = a_o + a_1 T_4 + a_2(T_4 - T_5) + a_3 \frac{T_4 - T_5}{\cos\theta} \quad \textit{with,} \;\; a_3 = \gamma W_o, \tag{4}$$

where W_o is the total column atmospheric water vapour from the sea surface to the satellite, and θ is the zenith viewing angle, ranging from 0^o at nadir to 72^o at the swath edges. For most applications and also for our study, the water vapour is an unknown quantity. Considering a constant a_3, (4) is identical with the NOAA split-window algorithm, which we will use for the retrieval of SST. The NOAA coefficients are listed in Annex A and they refer to [°C] for both the input brightness temperatures (T_4, T_5) and the retrieved SST (T_S).

Assuming that the difference of channel-4 and -5 brightness temperatures varies linearly with the water vapour over the total path length, one obtains from (4),

$$T_S = a_o + a_1 T_4 + a_2(T_4 - T_5) + a_3(T_4 - T_5)^2, \tag{5}$$

i.e. a quadratic approach with coefficients, which are independent of water vapour and look angle of the radiometer. Barton [3] suggests development of operational algorithms that include a quadratic term like (5). He claims that this was suggested 20 years ago [8] but no further algorithms of this kind have been reported until the recent work of Emery *et al.* [7].

3
Ground-truth data

For the comparison of satellite-retrieved and *in-situ* measured SST, it is essential that the data are from the same position and taken at the same time. Ground-truth data are available from ship measurements in the north Tyrrhenian Sea (south of Elba), south Adriatic Sea and Strait of Otranto, and from satellite-tracked drifters in the Adriatic and Ionian Sea and in the Nordic Seas (Greenland-Iceland-Norwegian Seas). Temporal coincidence of the satellite and drifter data is ensured by the fact that both are collected by the same satellite.

3.1 *Ship measurements*

SST has been recorded from onboard *NRV Alliance* by means of the ZENO-Alliance Network (ZAN), ZENO and ZAN being trade names of the Coastal Climate Company (USA). ZAN is a monitoring system designed specifically for shipboard installation [9]. The network integrates measurements of apparent wind, air temperature, relative humidity, barometric pressure and water temperature with information on ship location, course and heading. The water temperature is measured at about 2 m below sea level on the port side of *NRV Alliance* (2.5 m above her keel) with a Sea-Bird Electronics (SB-3) thermistor. The sensing elements extend about 40 cm off the hull, on the forward port side at the level of the bridge. Sampling is performed at 1 Hz and averages over 1 min (i.e. 60 samples) are taken. The ship's positions and SSTs are interpolated to a common time base with 5 min spacing. At full speed, *NRV Alliance* moves by some 1.6 km within 5 min, i.e. about the distance of an AVHRR resolution cell. Navigation information is available from the ship's differential GPS.

3.2 *Satellite-tracked drifters*

Since 1991, SACLANTCEN has deployed satellite-tracked drifters in the Nordic (Greenland-Iceland-Norwegian) and the Mediterranean (Adriatic and Ionian) Seas in order to measure the sea surface currents and SST in support of modelling and measurements of the variability of the acoustical environment. The drifter used in the Nordic Seas was the WOCE/TOGA drifter in which the surface fiberglass sphere houses a thermistor at 10 - 15 cm below sea level [10]. In the Mediterranean, a system similar to the CODE drifter [11] with a thermistor embedded in the main tubular hull at about 40 cm under the sea level was utilized. Both thermistors measure temperature with an accuracy of $\pm 0.1^{\circ}$C and resolution of about 0.05°C once a minute and an averaged temperature over 15 min is calculated.

SST data retrieval and location are made by the Argos Data Collection and Location System (DCLS) carried by the NOAA polar-orbiting satellites. During a satellite overpass, the drifter location is calculated from the Doppler shift of a fixed frequency signal emitted by the drifter every 90 s. SST is also telemetered at the same transmission rate. From all the temperatures obtained during a typical overpass of some 15 min, the median value is calculated and assigned to the drifter location. For some passes (with very low or very high elevation), the drifter position can not be calculated accurately from the Doppler shifts and no location is given by Argos while the SST is available.

4

Method of comparison

Satellite imagery yields synoptic views of SST. Over periods of only a few hours these structures may change considerably, e.g. being advected by surface currents. This has to be taken into account when comparing satellite and ground-truth data. In this memorandum we confine ourselves to data with the best possible coincidence in position and time. One source of ground-truth data are ship measurements. These are available from two cruises in spring 1995, to the Tyrrhenian and to the south Adriatic Sea. For the first cruise the satellite data have been purchased from the University of Dundee (UK), while for the second cruise the new *TeraScan* system was operated from onboard *NRV Alliance*. Because of the limited number of satellite overpasses and occasional cloud-coverage, the sets of coincident ship-borne and satellite measurements are small.

The second source of data are temperature measurements of satellite-tracked drifters. These are recorded by the Argos system onboard the same satellites which perform the AVHRR imagery. The main advantage of the drifter data is that they are available over a much longer period than the ship measurements, i.e. allow for better statistics. Most of the data analyzed are from the Adriatic and Ionian Sea, covering the period from May to July 1995. In addition, some data from the Nordic Seas waters are analyzed.

Satellite images from both sources, purchased from the University of Dundee (UK) and recorded by the *TeraScan* system, are processed by means of the *TeraScan* software. In order to ensure coincidence in position, the satellite images have to be correctly located. Small errors of up to some 10 km may occur due to the inaccuracy of the satellite's clock. As all data are from coastal areas this problem has been overcome by navigating the images against a map of coastlines. The *TeraScan* software provides automatic and manual routines, which have both been used for optimizing the alignment. Nevertheless, there remains an inaccuracy of the order of the AVHRR pixel size, i.e. some ± 1 km.

For each position of an *in-situ* measurement, coincident AVHRR data have been extracted from the satellite images by means of the *TeraScan* software, channel-4 and channel-5 for the retrieval of SST, channel-2 and channel-3 for the detection of cloud contamination. In order to apply the tests of Section 2.3, boxes of each 9 pixels have been collected. In addition, satellite and sun angles have been determined, the first is needed in the retrieval algorithm (4) and the second to distinguish between day- and night-time data. The importance of the different tests for cloud-masking is investigated. Following Flament [12], small clouds are identified by means of the variances within the boxes of both channel-2 and channel-4 data, instead of using absolute differences as the *Terascan* software. In accordance with the *TeraScan* routines, the correction for the atmosphere refers to the average over the box. Hence, the difference of channel-4 and channel-5 brightness temperatures in the retrieval algorithms (3) through (5) is,

$$T_4 - T_5 \equiv \frac{1}{9}\sum_{i=1}^{9}(T_{4i} - T_{5i}), \tag{6}$$

where the index i refers to the pixels of a box.

Even if the satellite and ground-truth data are from the same position and taken simultaneously, they may deviate. Satellite data refer to the uppermost millimetre of the surface (skin), wheras the drifter measurements are taken at about 40 cm below the sea surface and the ship measurements at 2 m (bulk temperatures). Because of the air-sea heat exchange surface skin temperature is generally several 0.1°C's colder than the bulk temperature. In addition, the satellite-retrieved temperatures represent spatial averages over at least 1 km^2, while *in-situ* temperatures are from point measurements.

In order to obtain quantitative results for the agreement of AVHRR-retrieved and *in-situ* measured SST, regression analyses are performed,

$$y = a_x x + y_0, \tag{7}$$

with the y-coordinate referring to the AVHRR and the x-coordinate to the *in-situ* data. The regression coefficients (a_x, y_0) are determined by the least-squares method, which minimizes the root-mean square (rms) error, given by,

$$\sigma = \sqrt{\frac{1}{N}\sum_{i=1}^{N}(y_i - a_x x_i - y_0)^2}, \tag{8}$$

where N is the number of measurements. This analysis is based on the assumption that the AVHRR data (y_i) account for most of the errors and the *in-situ* temperatures (x_i) are about exact. This assumption seems reasonable, because the AVHRR data are strongly affected by the atmosphere. In addition, we calculate the regression curve with the fixed slope $a_x = 1$ in (7),

$$y = x + b, \tag{9}$$

where $b = y_0$ represents the bias, i.e. the difference between the means of the satellite and *in-situ* temperatures.

5

Comparison with ship measurements

During an acoustic experiment in the Tyrrhenian Sea (south of Elba), from 19 April to 7 May 95, *NRV Alliance* collected near-surface water temperatures by means of the ZAN system. AHVRR data were purchased from the University of Dundee (UK) of NOAA-14 during daytime overpasses. For the period from 14 May to 24 May 95, *NRV Alliance* performed oceanographic measurements in the south Adriatic Sea and the Strait of Otranto. AVHRR data could be received from the NOAA-9, NOAA-12, and NOAA-14 satellites by means of the *TeraScan* system. Parts of the area were always cloud-covered, except for the last three days. Nevertheless, some data was collected for comparison with SST measurements, taken from the ship by means of the ZAN system, i.e. 2 m below the sea surface.

5.1 Comparison along ship-tracks

When comparing simultaneous ship- and satellite-measured SST only one data pair is available from each satellite overpass. This limits the number of data for a two-week experiment. However, there are no strong tides in the Mediterranean Sea areas considered and SST fields can expected to be stationary over the period of a few hours. For acoustic applications, it is of interest to know how well satellite-imagery can resolve the spatial variability of SST, i.e. the SST gradients. In addition to a cloud-free sky, the comparison with ground-truth data requires that the ship has moved over a certain distance with strong temperature gradients present. For each of the two experiments we found only one case where these requirements are fulfilled.

Figure 1 displays selected AVHRR image from the Tyrrhenian Sea (south of Elba), together with locations of *NRV Alliance* from 40 min before to 50 min after the satellite overpass. The channel-4 brightness temperature reveals strong spatial variability. Times, positions, ship- and satellite-measured temperatures are listed in Table B1 of Annex B. Ship-measured SST and channel-4 brightness temperatures vary by almost 3°C. However, the regression analysis presented in Fig. 2 shows a relatively poor agreement between ship- and satellite-measured temperatures. For determining SST from the satellite data, the split-window algorithm (4) has been applied with the NOAA coefficients (Table A1 in Annex A). The rms error σ for the channel-4 temperatures is smaller than that for the retrieved SST. The bias of 1.2°C is unexpectedly high.

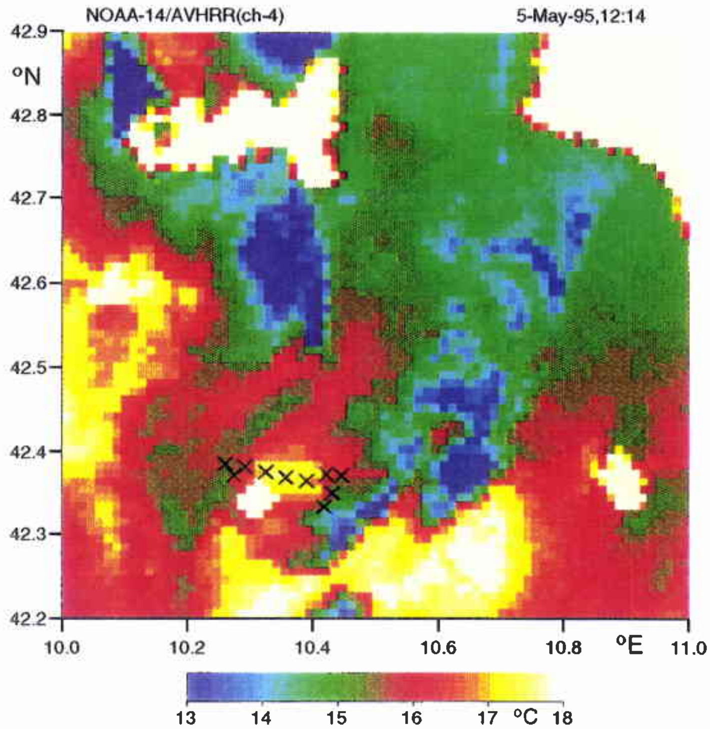

Figure 1: *AVHRR (channel-4) brightness temperatures in the Tyrrhenian Sea (south of Elba). The crosses mark positions of NRV Alliance from about 40 min before to 50 min after the satellite overpass.*

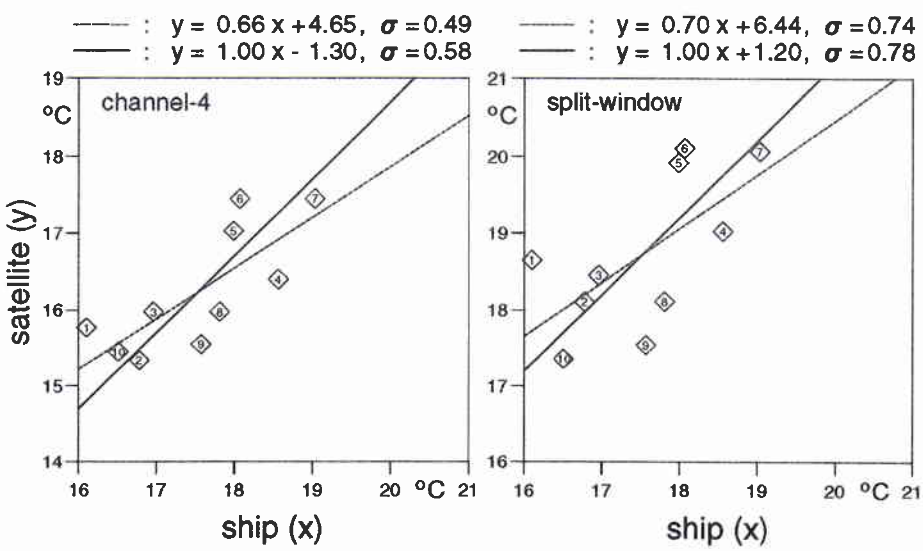

Figure 2: *Comparison of satellite- and ship-measured temperatures at the positions indicated in Fig. 1. The numbers refer to the data of Table B1 in Annex B. Left panel: brightness temperatures. Right panel: retrieved SSTs.*

Due to extensive CTD measurements the selected track of *NRV Alliance* in the Adriatic Sea extended over a longer time period, from 2.5 h before to 2.0 h after the satellite overpass. The channel-4 brightness temperatues are displayed in Fig. 3. Times and coordinates of the positions, shown in Fig. 3, and ship- and satellite measured temperatures are listed in Table B2 of Annex B. In contrast to the Elba data, Fig. 4 shows an excellent agreement of ship-measured and satellite-retrieved temperatures. There is almost no bias and the rms error is only 0.25°C.

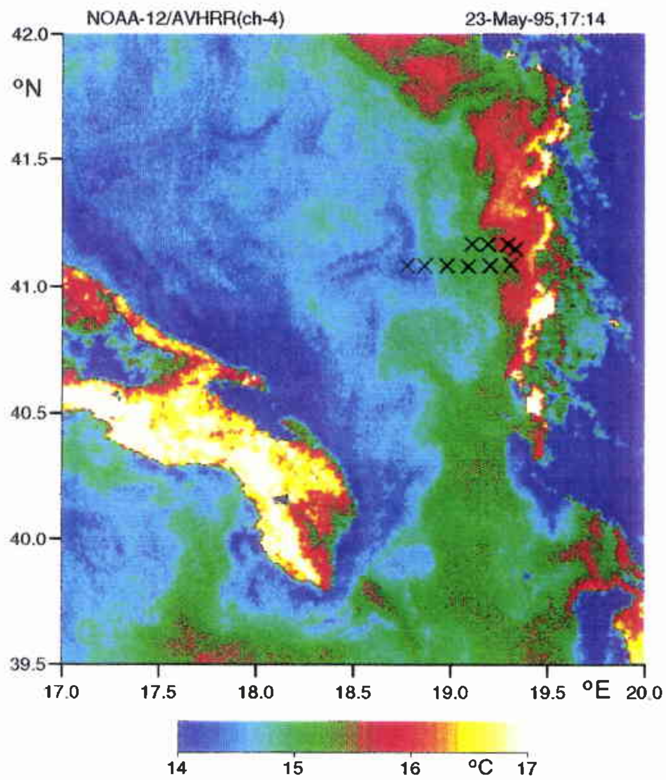

Figure 3: *AVHRR (channel-4) brightness temperatures in the south Adriatic Sea. The crosses mark positions of NRV Alliance.*

When comparing both examples we find that the satellite zenith angle for both images is small, 15° for the Elba image (Fig. 1) and 24° for the Adriatic image (Fig. 3). The albedo is 2.1% and 0.6%, respecively, i.e. higher for the Elba data. But this value is below the threshold given in Section 2.3, and should not cause the discrepencies observed. The standard deviation of the Elba channel-2 data within the boxes does not indicate the presence of small clouds. However, the standard deviation of the channel-4 data is high, and as described in Section 2.3, nearly all of the data should be discarded because of possible contamination by small clouds. From the ship measurements it is obvious that not clouds but SST variability causes the high rms error in Fig. 2. Hence, the SST short-scale variability in conjunction with inaccuracies of the location of the satellite data must be the major cause of error.

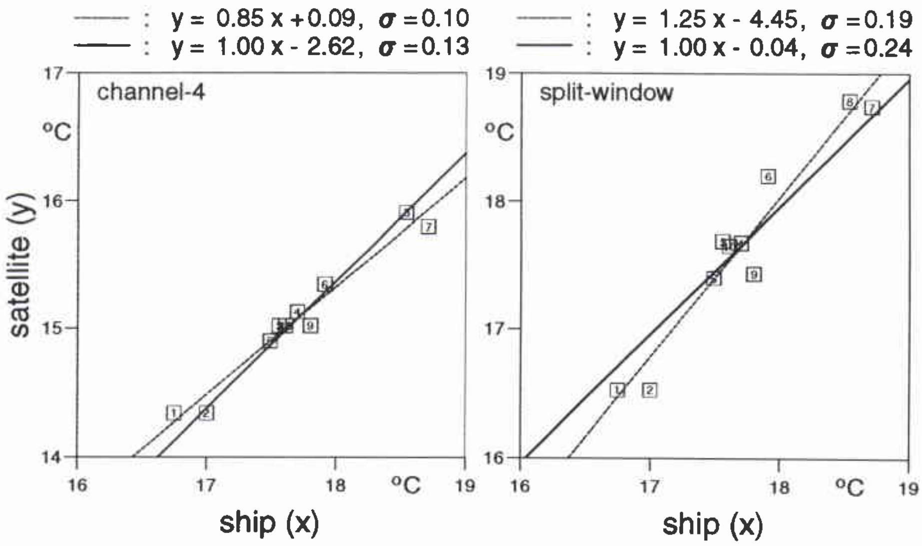

Figure 4: ***Comparison of satellite- and ship-measured temperatures at the positions indicated in Fig. 3. The numbers refer to the data of Table B2 in Annex B. Left panel: brightness temperatures. Right panel: retrieved SSTs.***

5.2 Comparison of coincident data

Images from both cruises have been selected in which the position of *NVR Alliance* is apparently cloud-free. SST has been computed by means of the split-window algorithm (4) with the NOAA coefficients (Table A1 in Annex A) and compared with the ship-measured SST (Fig. 5). The diamond symbols refer to data from the Tyrrhenian Sea, the square symbols to data from the Adriatic Sea. Night-time data are indicated by bold frames, and the respective number of the NOAA satellite is given. Left and right panels deviate by the number of data considered, which is determined by the thresholds for cloud detection. The upper limit for the channel-2 albedo has been decreased from 5% to 3% and that for the channel-4 standard deviation from 0.3°C to 0.15°C. The other tests are the same for both panels, data with channel-4 temperatures below 10°C and from zenith angles greater than 60° have not been considered. Daytime data with channel-2 standard deviation greater than 0.3% and night-time data with a difference between channel-3 and channel-4 of less than -1.5°C have been discarded.

With respect to the rms error the higher requirements for cloud masking lead to a considerable improvement. But this is mainly due the elimination of the one data point at which the satellite SST deviates by nearly 2°C from the regression curve

(Fig. 5, left panel). This point is from the Elba experiment and fails the higher requirement for the channel-4 variance. All the other missing points have been discarded because their channel-2 albedo exceeds 3%.

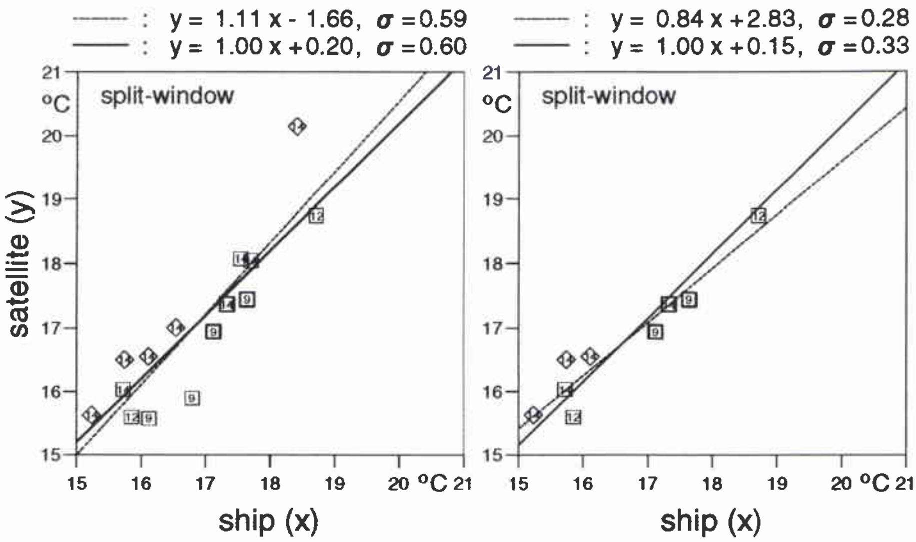

Figure 5: *Comparison of coincident satellite- and ship-measured SST during the cruises in the Tyrrhenian Sea (diamonds) and south Adriatic Sea (squares). Bold squares indicate night-time data. Thresholds for the channel-2 albedo are 5% and 3% and for the channel-4 standard deviation 0.3°C and 0.15°C in the left and right panel, respectively.*

6

Comparison with drifter data

Data for comparison of SST, as measured by satellite-tracked drifters and retrieved from the AVHRR, are available from two different areas: the Nordic Seas (Greenland-Iceland-Norwegian Seas) and the Mediterranean (Adriatic and Ionian Seas). An algorithm (4) is used to determine SST from channel-4 and channel-5 brightness temperatures, with NOAA coefficients (Table A1 in Annex A).

6.1 Nordic Seas

Five AVHRR images were selected from the period April to September 1993 for the comparison of satellite- and drifter-measured SST in the Nordic Seas. The images were purchased from the University of Dundee (UK), they were all taken during daytime and are from NOAA-11. Drifter data have been collected from the area between 62°N and 77°N and between 13°W and 19°E. Results of the comparison are presented in Fig. 6. Left and right panels differ by the number of data points considered, which depends on the thresholds used for cloud detection.

For both panels in Fig. 6, data have been rejected if their channel-4 brightness temperatures are below -2°C, or if their zenith angles exceed 60°, or if their channel-2 variances are above 0.3%. Upper limits for the channel-2 albedo are 5% in the left panel and 3% in the right panel, bounds for the channel-4 standard deviation are 0.3^oC and 0.1^oC, respectively. Mainly due to the stronger requirement for the channel-4 smoothness, the data points decrease from 37 to 26. However, there is only little reduction of the rms error. Further experiments with the thresholds show that better fits are not obtainable, mainly due to the fact that the NOAA coefficients are not optimal for the data under consideration.

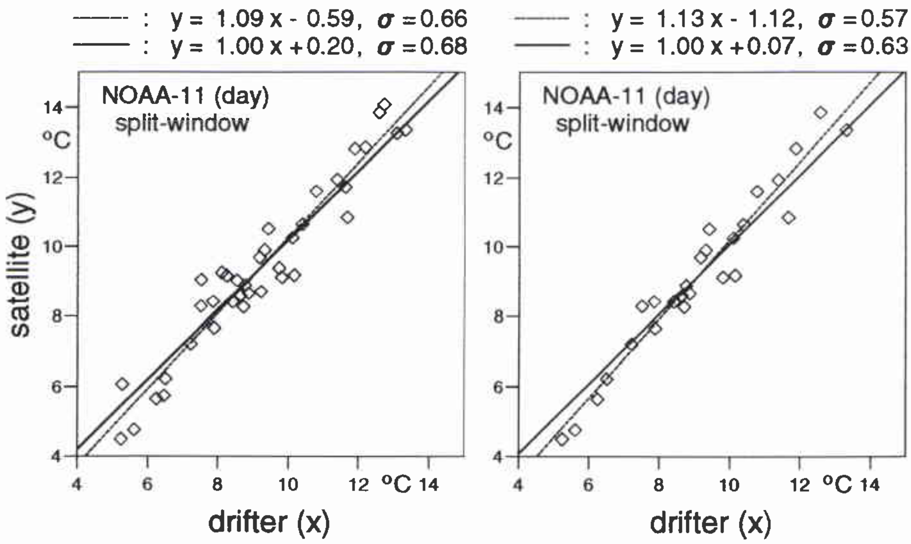

Figure 6: *Comparison of coincident satellite- and drifter-measured SST from the Greenland-Iceland-Norwegian Seas. Thresholds for the channel-2 albedo are 5% and 3% and for the channel-4 standard deviation 0.3°C and 0.1°C in the left and right panel, respectively.*

6.2 Mediterranean

The data investigated were collected during the period May to July 1995, most of them in the Adriatic Sea and some in the Ionian Sea. The AVHRR data are from NOAA-12 and NOAA-14, both of which tracked the drifters. Due to the orbit of the satellite, no night-time data of NOAA-12 could be acquired. Figures 7-9 compare drifter- and satellite-measured SST, separately for the two satellites and for day- and night-time. Again, left and right panels differ by the number of data points, determined by deviating thresholds for cloud detection.

In order to eliminate unreliable points, AVHRR data with channel-4 brightness temperatures below 10°C or from zenith angles greater than 60° are not considered. Night-time data are rejected if the difference between channel-3 and channel-4 brightness temperatures falls below -1.5°C. It has been found that, for daytime data, the lowering of the thresholds for the channel-2 albedo and the channel-2 standard deviation is of little influence. Bounds of 5% and 0.3%, respectively, have been applied for both panels in Figs. 7-9. Thus, the only threshold varied is the channel-4 standard deviation, which is 0.3°C for the left and 0.1°C for the right panels.

By lowering the threshold for the channel-4 standard deviation, the rms error of the NOAA-12 daytime data decreases considerably from 0.67°C to 0.45°C (Fig. 7), while the small bias of 0.15°C remains unchanged. In Fig. 8, which reveals the comparison with NOAA-14 daytime data, both the rms error of 0.46°C and the bias of 0.55°C change only slightly by introducing a lower bound for the channel-4 standard deviation. The bias is rather high and does not allow reliable retrieval of SST. The lower bound for the channel-4 standard deviation with the NOAA-14 night-time data yields no improvement (Fig. 9). But in this case there is nearly no bias and the rms error of 0.36°C is satisfactory.

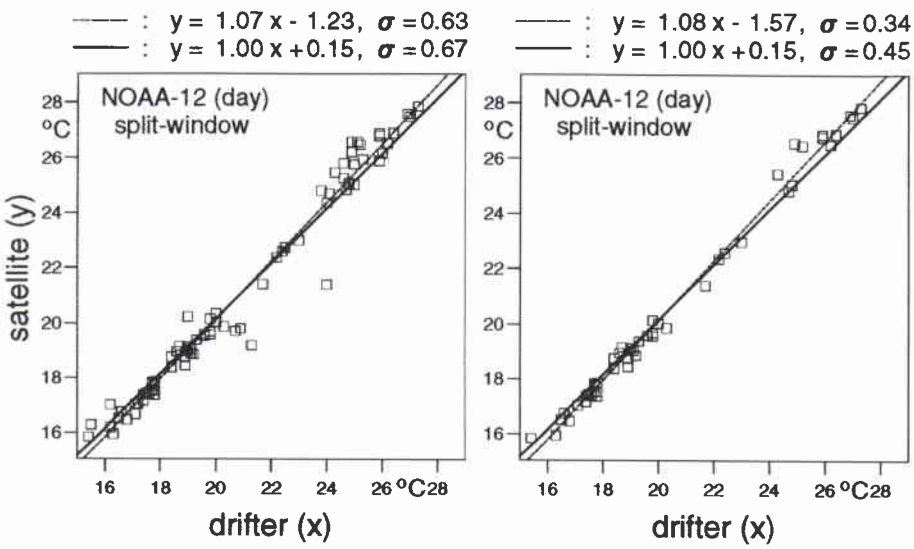

Figure 7: *Comparison of coincident satellite- and drifter-measured SST from the south Adriatic and Ionian Sea. The day-time satellite data have been taken from NOAA-12 from May to July 1995. Thresholds for the channel-4 standard deviation are 0.3°C and 0.1°C in the left and right panel, respectively.*

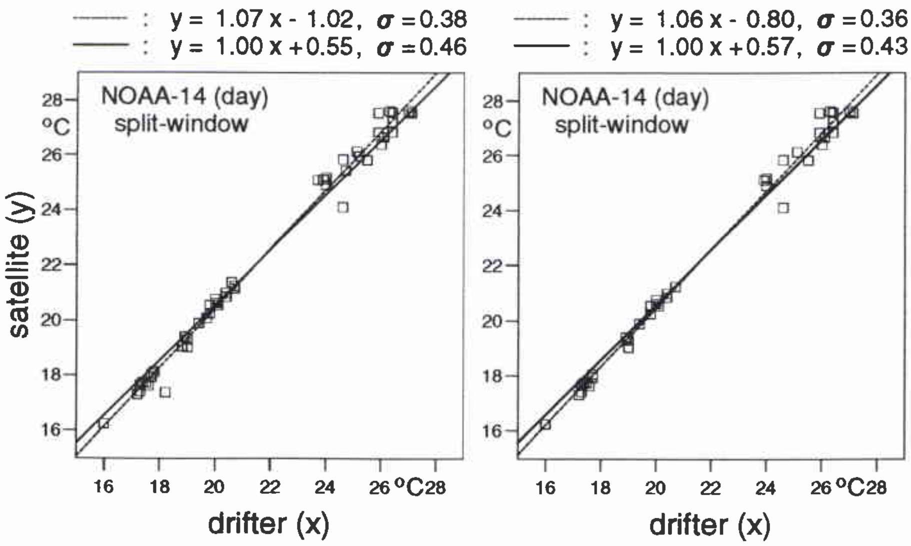

Figure 8: *Comparison of coincident satellite- and drifter-measured SST from the south Adriatic and Ionian Sea. The day-time satellite data have been taken from NOAA-14 from May to July 1995. Thresholds for the channel-4 standard deviation are 0.3°C and 0.1°C in the left and right panel, respectively.*

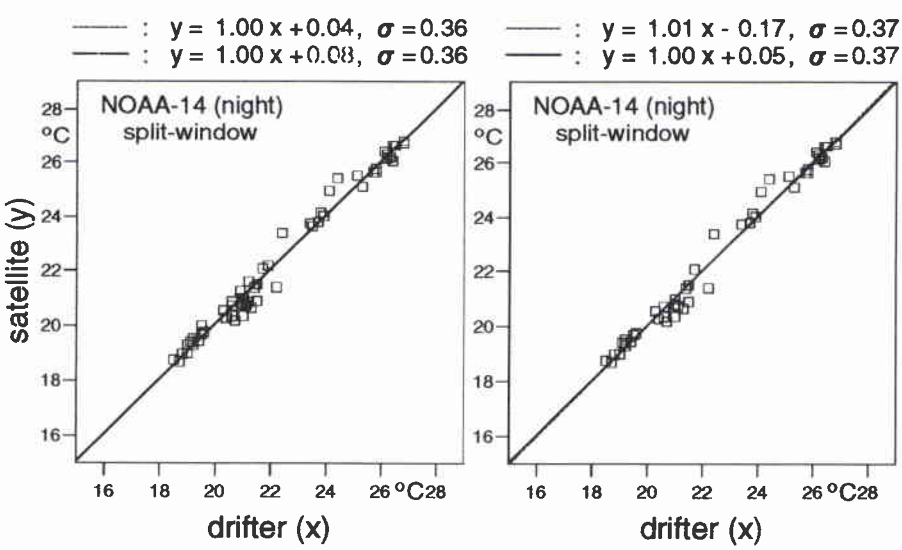

Figure 9: *Comparison of coincident satellite- and drifter-measured SST from the south Adriatic and Ionian Sea. The night-time satellite data have been taken from NOAA-14 from May to July 1995. Thresholds for the channel-4 standard deviation are 0.3°C and 0.1°C in the left and right panel, respectively.*

7

Test of algorithms

Using drifter data we investigate the impact of the functional form of the retrieval algorithm. We confine ourselves to the equations (3)-(5), which all are based on channel-4 and channel-5 data only. In the previous chapters, algorithm (4) has been used for retrieval with coefficients supplied by NOAA. Algorithm (3) ignores the dependence on the viewing angle of the radiometer and represents the simplest split-window method. Nevertheless, many examples in the literature show its utility. Though the algorithm (5) contains no explicit angle-dependence this may be included implicitly in the quadratic term.

For the following investigations we determine the coefficients of the three algorithms (3)-(5), by means of a least-squares fit, from the data available. We then use these matched formulas to calculate the bias and rms error of the retrieved *versus* the ground-truth data. The result represents the best possible fit for the respective algorithm, and the values of bias and rms error define the quality of the algorithm. The coefficients found from the different data sets are listed in Annex C. The results of the regression analysis are shown in the following figures, where for the presentation we confine ourselves to regression lines of slope 1, equation (9).

Figure 10 displays results for the data from the Nordic Seas. Thresholds for cloud detection are the same as used for the left panel of Fig. 6. More restrictive bounds do not alter the results with respect to the rms error σ. Compared with Fig. 6, it may be stated that in principle, a more accurate determination of SST is possible than with the NOAA coefficients. Surprisingly, all three algorithms (3)-(5) yield about the same good fits. The consideration of the satellite look angle leads to no improvement, even though the zenith angles of the satellite data are nearly uniformly distributed in the interval $[0°, 50°]$. The matched coefficients nearly totally suppress the bias.

Results for the data from the Adriatic and Ionian Sea are shown in Fig. 11. Thresholds for cloud detection are the same as used in the right panels of Figs. 7-9, i.e. the lower bound for the channel-4 variance is applied, which allows a decrease in the rms error σ of the NOAA-12 daytime data (Fig. 7). By comparing the upper panel of Fig. 11 with the right panel of Fig. 7, a decrease of the rms error from 0.45°C to 0.31°C is found. The three algorithms (3)-(5) yield similar results. The middle panel of Fig. 11 corresponds to the right panel of Fig. 8 and refers to the NOAA-14 daytime data. Here the algorithm (4), which makes use of the satellite viewing angle, is superior. The same holds for the NOAA-14 night-time data, cf. lower panel of Fig. 11, which corresponds to the right panel of Fig. 9.

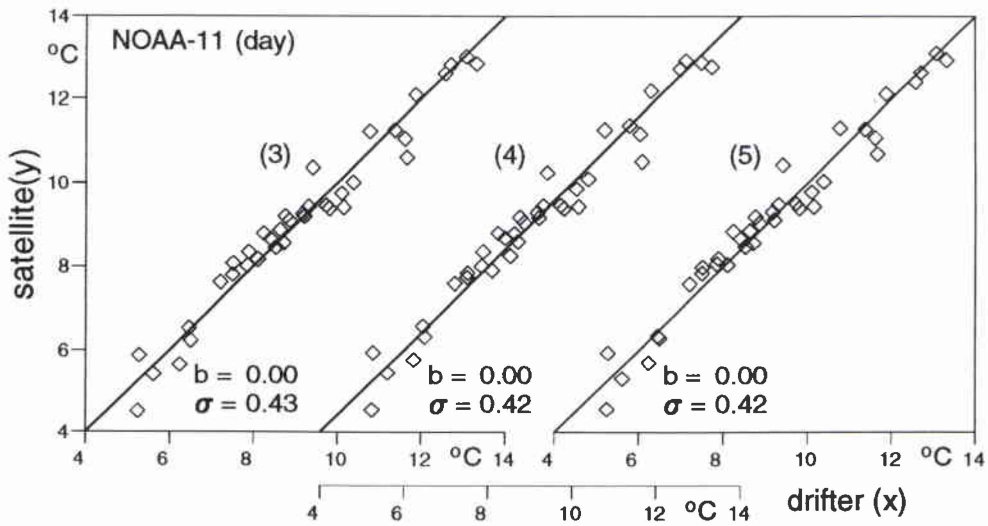

Figure 10: *Comparison of coincident satellite- and drifter-measured SST from the Greenland-Iceland-Norwegian Seas. Matched coefficients are used for the algorithms (3)-(5). The thresholds for cloud detection are those of Fig. 6, left panel.*

By investigating the zenith angles of the satellite data used, it is found that the portion of large angles is higher for both the NOAA-14 day- and night-time data than for the NOAA-12 data. This explains the different results with respect to the importance of the zenith-angle dependence in retrieval algorithms. When considering data from zenith angles of less than e.g. 40° only, the zenith-angle dependence may be neglected. This is demonstrated by Fig. 12, which merges the data from both satellites, NOAA-12 and NOAA-14 as well as day- and night-time data. Another conclusion from Fig. 12 is that one set of coefficients allows a satisfactory retrieval of SST from both satellites.

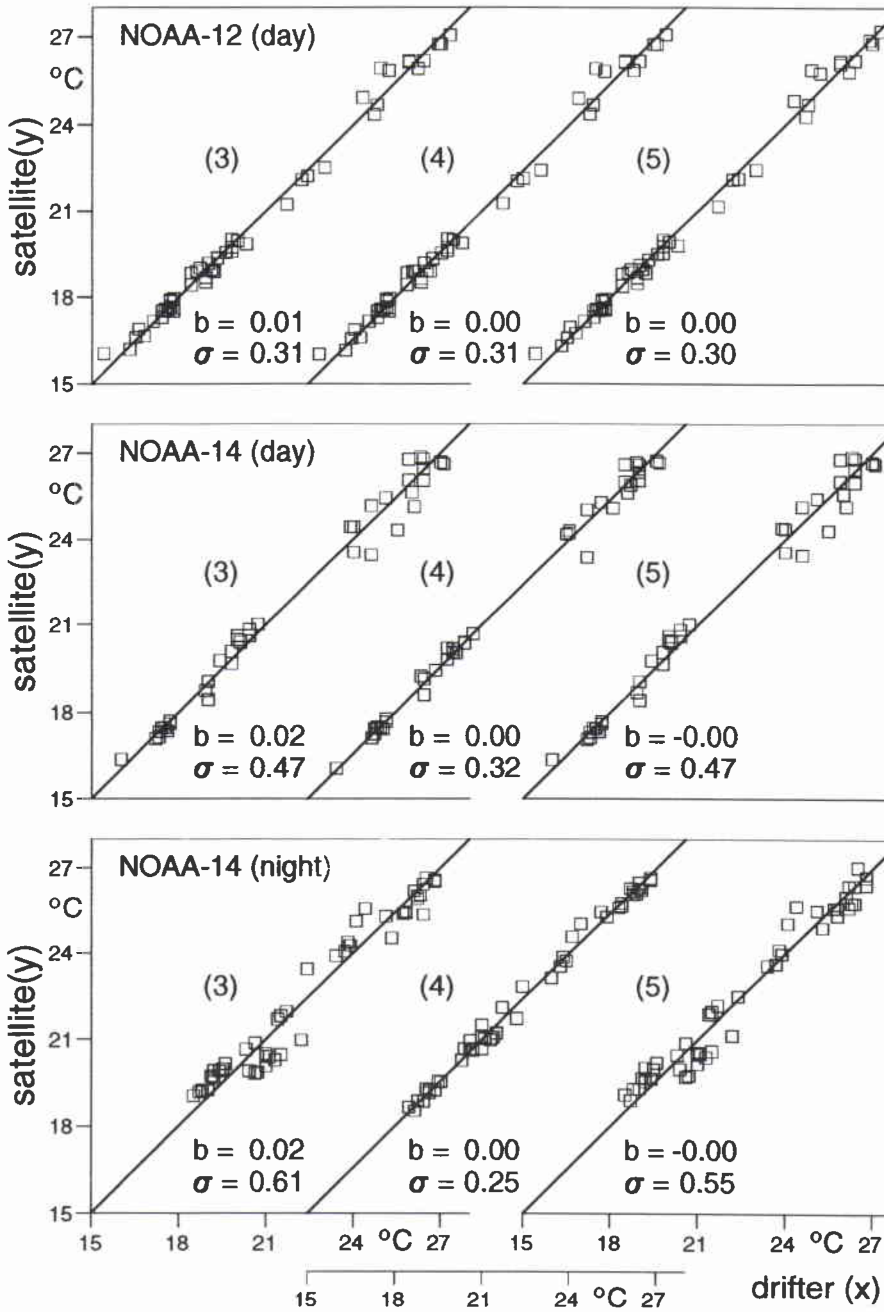

Figure 11: *Comparison of coincident satellite- and drifter-measured SST from the Adriatic and Ionian Seas. Matched coefficients are used for the algorithms (3)-(5). The thresholds for cloud detection are those of Figs. 7-9, right panels.*

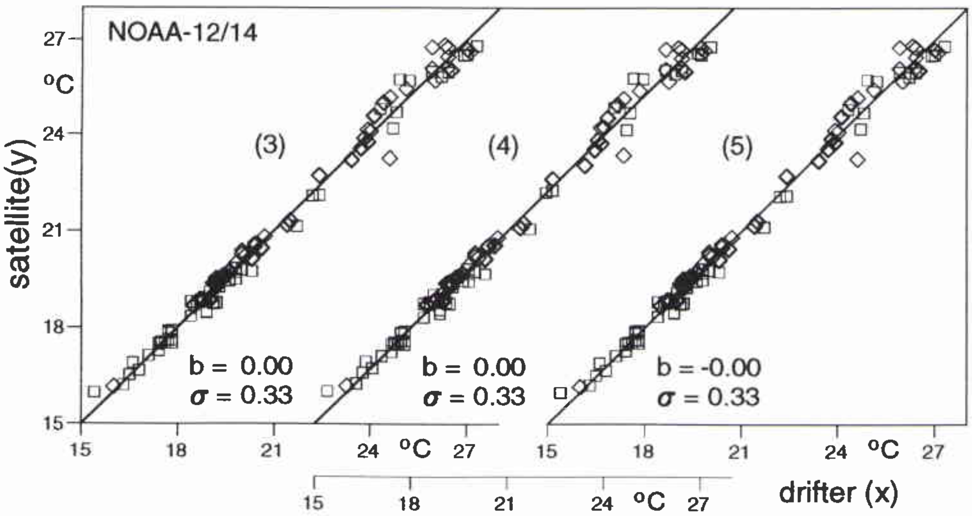

Figure 12: *Comparison of coincident satellite- and drifter-measured SST from the Adriatic and Ionian Seas. Satellite measurements from zenith angles less than 40° from both satellites, NOAA-12 (squares) and NOAA-14 (diamonds), are considered. Night-data are indicated by bold frames. Matched coefficients are used for the algorithms (3)-(5). The thresholds for cloud detection are the same as in Fig. 11.*

8 Conclusions

Satellite-retrieved SST has been compared with *in-situ* data from ship and drifter measurements, about 2 m and 0.4 m below the sea surface, respectively. Most of the data are from the Mediterranean and some from the Nordic Seas. The calibration and location of the satellite data have been performed by the *TeraScan* software, as well as the extraction of data needed for the comparison. For retrieval, a split-window algorithm has been used with coefficients supplied by NOAA for global application. The agreement between satellite-retrieved and *in-situ* measurement differs considerably for the data sets investigated. Biases of up to 0.6°C and rms errors of up to 0.7°C have been found by means of regression analyses.

The elimination of noise- and cloud-contaminated pixels is essential for obtaining reliable SSTs from satellite measurements. Pixels viewed under zenith angles greater than 60° should be discarded. For daytime data, upper bounds of 5% for the channel-2 albedo and 0.3% for its standard deviation are found to be sufficient. By reducing these values, no significant improvement of the rms error could be achieved. Night-time data are rejected if the difference between channel-3 and channel-4 brightness temperature falls below -1.5°C. For some data sets, the decrease of the upper bound for the channel-4 standard deviation from 0.3°C to 0.1°C yields lower rms errors. It should be noted that this procedure not only eliminates data contaminated by small clouds but also data from areas with strong horizontal gradients of SST. Due to insufficient resolution or inaccurate location, the respective satellite-retrieved SSTs may also be erroneous.

By means of matched coefficients, i.e. determined from the data, retrieval algorithms reveal a better performance, with vanishing bias and rms errors less than 0.4°C. This means that regional algorithms should be advantageous compared with the global NOAA algorithm. The consideration of viewing angle by a retrieval algorithm becomes important if data are involved, which have been received from zenith angles larger than some 40°. The quadratic algorithm (5) does not reveal advantages for any of the data sets investigated.

References

[1] Siegel, H., Gerth, M., Rudloff, R., Tschersich, G. (1994). Dynamic features in the western Baltic Sea investigated using NOAA-AVHRR data. *Deutsche Hydrographische Zeitschrift*, **46**, 191-209.

[2] McClain, E.P., Pichel, W.G., Walton, C.C. (1985). Comparative performance of AVHRR-based multichannel sea surface temperatures. *Journal of Geophysical Research*, **90**, 11587-11601.

[3] Barton, I.J. (1995). Satellite-derived sea surface temperatures: current status. *Journal of Geophysical Research*, **100**, 8777-8790.

[4] Minnett, P.J, Saunders, R.W., Nacini, E. (1995). Ship and aircraft validation of AVHRR skin and bulk sea-surface temperature retrievals in the Eastern Mediterranean. Unpublished manuscript.

[5] Kidwell, K.B. (1991). NOAA polar orbiter data users guide. NOAA National Environmental Satellite, Data, and Information Service, Washington D.C., USA.

[6] Minnett, P.J. (1990) The regional optimization of infrared measurements of se-surface temperature from space. *Journal of Geophysical Research*, **95**, 13497-13510.

[7] Emery, W.J., Yu, Y., Wick, G.A., Schluessel, P., Reynolds, R.W. (1994). Correcting infrared satellite estimates of sea surface temperature for atmospheric water vapor attenuation. *Journal of Geophysical Research*, **99**, 5219-5236.

[8] McMillin, L.M. (1975). Estimation of sea surface temperatures from two infrared window measurements with different absorption. *Journal of Geophysical Research*, **80**, 5113-5117.

[9] Minnett, P.J. (1991). Surface measurements made during the Icelandic Current Experiment (ICE 89) from the R/V Alliance, SACLANTCEN SM-247. La Spezia, Italy, NATO SACLANT Undersea Research Centre.

[10] Poulain, P.-M., Warn-Varnas, A., Niiler, P.P. (1995). Near-surface circulation of the Nordic Seas as measured by Lagrangian drifters. *Journal of Geophysical Research*, accepted.

[11] Davis, R.E. (1985). Drifter observations of coastal surface currents during CODE: The method and descriptive view. *Journal of Geophysical Research*, **90**, 4741-4755.

[12] Flament, P. (1995). Personnel communication. University of Hawaii.

A

NOAA coefficients of the split-window algorithm

For the operational generation of SST maps, NOAA applies different algorithms (Kidwell, 1991). The so-called linear MCSST is a split-window algorithm, i.e. it makes use of channel-4 and channel-5, and is identical with (3) for NOAA-9 and with (4) for the following satellites (a_3 = *constant*). The coefficients are derived from a regression analysis using coincident satellite and drifting buoy data. A global accuracy of 0.7°C is claimed for this algorithm [3]. The NOAA-coefficients as defined by (4), with all temperatures in [°C], are presented in Table A1.

satellite	time	a_o	a_1	a_2	a_3
NOAA-9	day	0.323	0.9731	2.6353	0.0
NOAA-9	night	0.982	0.9936	2.6900	0.0
NOAA-11	day	-0.918	1.0135	2.1332	0.52655
NOAA-11	night	-1.317	1.0520	1.4373	0.95977
NOAA-12	day	-0.912	1.0137	2.1292	0.31431
NOAA-12	night	-0.912	1.0137	2.1292	0.31431
NOAA-14	day	-0.543	1.0173	1.3599	0.77971
NOAA-14	night	-1.145	1.0291	1.5228	0.75257

Table A1: *NOAA coefficients of the retrieval algorithm (4).*

B

Ship- and satellite- measured SST

This annex contains times and positions of *NRV Alliance* along the two sections investigated, south of Elba (Table B1) and in the south Adriatic Sea (Table B2). Also given are the ship-measured SST, channel-4 brightness temperature (T_4), its standard deviation within a box of 3 × 3 pixels (σ_4) and the SST determined by the split-window alorithm (T_s).

No.	time	lat.	long.	SST	T_4	σ_4	T_s
1	11:33	42.332	10.418	16.1	15.8	0.67	18.4
2	11:43	42.349	10.431	16.8	15.3	0.31	17.9
3	12:53	42.370	10.446	17.0	16.0	0.20	18.2
4	12:03	42.372	10.422	18.6	16.4	0.22	18.8
5	12:13	42.364	10.390	18.0	17.0	0.15	19.7
6	12:23	42.368	10.357	18.1	17.5	0.22	19.9
7	12:33	42.375	10.325	19.0	17.5	0.35	19.8
8	12:43	42.381	10.293	17.8	16.0	0.35	17.9
9	12:53	42.385	10.261	17.6	15.6	0.09	17.3
10	13:03	42.371	10.275	16.5	15.4	0.14	17.1

Table B1: *Time, position, ship- and satellite-measured SST along the section of NRV Alliance south of Elba, 5-May-95 (Fig. 1).*

No.	time	lat.	long.	SST	T_4	σ_4	T_s
1	14:48	41.083	18.775	16.8	14.3	0.05	16.5
2	15:08	41.083	18.865	17.0	14.3	0.05	16.5
3	15.33	41.083	18.977	17.6	15.0	0.06	17.7
4	15:58	41.081	19.088	17.7	15.1	0.05	17.7
5	16:23	41.083	19.200	17.5	14.9	0.05	17.4
6	16:48	41.087	19.307	17.9	15.4	0.12	18.2
7	17:18	41.148	19.330	18.7	15.8	0.07	18.7
8	17:58	41.167	19.291	18.5	15.9	0.09	18.8
9	18:38	41.167	19.190	17.8	15.0	0.09	17.4
10	19:23	41.167	19.106	17.6	15.0	0.04	17.7

Table B2: *Time, position, ship- and satellite-measured SST along the section of NRV Alliance in the south Adriatic Sea, 23-May-95 (Fig. 3).*

C

Empirical coefficients of the split-window algorithm

This annex summarizes the coefficients which have been found by fitting the data of Section 7 against the three algorithms (3) - (5).

data	algorithm	a_o	a_1	a_2	a_3
a	(3)	0.0	0.979	1.464	
a	(4)	0.121	0.965	2.794	-1.206
a	(5)	-0.152	0.983	2.049	-0.432
b	(3)	0.773	0.939	2.125	
b	(4)	0.681	0.940	2.446	-0.254
b	(5)	2.411	0.934	-0.059	0.743
c	(3)	0.829	0.926	2.198	
c	(4)	0.979	0.950	0.696	0.928
c	(5)	-0.246	0.928	3.318	-0.303
d	(3)	0.536	0.975	2.073	
d	(4)	-0.193	0.992	0.539	1.373
d	(5)	-6.863	1.035	9.179	-1.933
e	(3)	1.079	0.940	1.836	
e	(4)	1.175	0.940	1.195	0.532
e	(5)	1.083	0.940	1.831	0.001

Table C1: *Coefficients of algorithms (3) - (5), derived by least-square fits of the data, a: Fig. 10, b: Fig. 11 (upper panel), c: Fig. 11 (middle panel), d: Fig. 11 (lower panel), e: Fig. 12.*

Report no. changed (Mar 2006): SM-297-UU

Document Data Sheet

NATO UNCLASSIFIED

Security Classification		Project No.
NATO UNCLASSIFIED		23
Document Serial No.	**Date of Issue**	**Total Pages**
SM-297	January 1996	35pp.

Author(s)

H.-H. Essen, E. Nacini, P.-M. Poulain

Title

Comparison of satellite-retrieved sea-surface temperatures with drifter- and ship-borne measurements.

Abstract

Sea-surface temperatures (SST) retrieved from satellite imagery are compared with *in-situ* measured data. The satellite data are from the Advanced Very High Resolution Radiometer (AVHRR) of the series of NOAA satellites, partly purchased from the University of Dundee (UK) or recorded by the new high-resolution receiver of SACALNTCEN, a *TeraScan* system (SeaSpace Corp., USA). Both data sets have been processed by the *TeraScan* software. The ground-truth data are from satellite-tracked drifters and from measurements onboard NRV *Alliance*. The aim of this memorandum is to determine the performance of the *TeraScan* system with respect to the accuracy of retrieved SST.

For reliably determining SST from the AVHRR, two steps have to be performed. First, cloud-contaminated data have to be removed and second, the measured brightness temperatures have to be corrected for atmospheric effects. The impact of these procedures on the accuracy of satellite-measured SST is investigated.

Keywords

Mediterranean – Nordic Seas – satellite imagery – sea-surface temperature – *TeraScan* system

Issuing Organization

North Atlantic Treaty Organization
SACLANT Undersea Research Centre
Viale San Bartolomeo 400, 19138 La Spezia, Italy

[From N. America: SACLANTCEN CMR-426 (New York) APO AE 09613]

Tel: +39 (0)187 540 111
Fax:+39 (0)187 524 600

E-mail: library@saclantc.nato.int

NATO UNCLASSIFIED

Initial Distribution for SM-297

SCNR for SACLANTCEN		*National Liaison Officers*	
SCNR Belgium	1	NLO Canada	1
SCNR Canada	1	NLO Denmark	1
SCNR Denmark	1	NLO Germany	1
SCNR Germany	1	NLO Italy	2
SCNR Greece	2	NLO Netherlands	1
SCNR Italy	1	NLO UK	3
SCNR Netherlands	1	NLO US	4
SCNR Norway	1		
SCNR Portugal	1		
SCNR Spain	1		
SCNR Turkey	1		
SCNR UK	1		
SCNR US	2		
French Delegate	1		
SECGEN Rep. SCNR	1	Total external distribution	34
NAMILCOM Rep. SCNR	1	SACLANTCEN Library	26
SACLANT	3	Total number of copies	60